Supporting Information

Table S1. (n,m) resolved SWNTs synthesized on Fe catalyst using CO at 800 ^{o}C.

Indices (n,m)	Diameter (nm)	Chiral angle (^{o})	Metallic/Semiconducting
(7,3)	0.70	17.0	S
(6,5)	0.75	27.0	S
(6,5)	0.75	27.0	S
(7,4)	0.76	21.1	M
(7,4)	0.76	21.1	M
(7,4)	0.76	21.1	M
(7,4)	0.76	21.1	M
(7,4)	0.76	21.1	M
(8,3)	0.77	15.3	S
(9,2)	0.80	9.8	S
(6,6)	0.81	30	M
(6,6)	0.81	30	M
(6,6)	0.81	30	M
(7,5)	0.82	24.5	S
(7,5)	0.82	24.5	S
(7,5)	0.82	24.5	S
(7,5)	0.82	24.5	S
(8,4)	0.83	19.1	S
(8,4)	0.83	19.1	S
(8,4)	0.83	19.1	S
(8,4)	0.83	19.1	S
(8,4)	0.83	19.1	S
(8,4)	0.83	19.1	S
(10,2)	0.87	8.9	S
(7,6)	0.88	27.5	S
(7,6)	0.88	27.5	S
(7,6)	0.88	27.5	S
(7,6)	0.88	27.5	S
(9,4)	0.90	17.5	S
(10,3)	0.92	12.7	S
(12,0)	0.94	0	M
(7,7)	0.95	30	M
(7,7)	0.95	30	M
(11,2)	0.95	8.2	M
(8,6)	0.95	25.3	S
(8,6)	0.95	25.3	S
(8,6)	0.95	25.3	S
(8,6)	0.95	25.3	S
(8,6)	0.95	25.3	S
(8,6)	0.95	25.3	S
(8,6)	0.95	25.3	S
(8,6)	0.95	25.3	S
(9,5)	0.96	20.6	S

(9,5)	0.96	20.6	S
(9,5)	0.96	20.6	S
(9,5)	0.96	20.6	S
(11,3)	1.00	11.7	S
(9,6)	1.02	23.4	M
(9,6)	1.02	23.4	M
(9,6)	1.02	23.4	M
(10,5)	1.04	19.1	S
(10,5)	1.04	19.1	S
(10,5)	1.04	19.1	S
(10,5)	1.04	19.1	S
(11,4)	1.05	14.9	S
(8,8)	1.09	30	M
(8,8)	1.09	30	M
(8,8)	1.09	30	M
(9,7)	1.09	25.9	S
(9,7)	1.09	25.9	S
(9,7)	1.09	25.9	S
(9,7)	1.09	25.9	S
(9,7)	1.09	25.9	S
(9,7)	1.09	25.9	S
(9,7)	1.09	25.9	S
(9,7)	1.09	25.9	S
(10,6)	1.10	21.8	S
(10,6)	1.10	21.8	S
(10,6)	1.10	21.8	S
(14,0)	1.10	0	S
(9,8)	1.15	28.1	S
(9,8)	1.15	28.1	S
(10,7)	1.16	24.2	M
(10,7)	1.16	24.2	M
(11,6)	1.17	20.4	S
(13,4)	1.21	13.0	M
(9,9)	1.22	30	M
(11,7)	1.23	22.7	S
(12,6)	1.24	19.1	M
(15,2)	1.26	6.2	S
(13,5)	1.26	15.6	S
(13,5)	1.26	15.6	M
(10,9)	1.29	28.3	S
(11,8)	1.29	24.8	M
(14,5)	1.34	14.7	M
(11,9)	1.36	26.7	S
(11,9)	1.36	26.7	S
(17,2)	1.42	5.5	M
(11,11)	1.49	30	M
(12,10)	1.50	27.0	S
(16,6)	1.54	15.3	S
(12,11)	1.56	28.6	S

(19,2)	1.57	4.95	S
(15,8)	1.58	20.0	S

Table S2. (n,m) resolved SWNTs synthesized on Fe catalyst using CH_4 at 800 ^oC.

Indices (n,m)	**Diameter (nm)**	**Chiral angle (^{o})**	**Metallic/Semiconducting**
(9,7)	1.09	25.9	S
(12,4)	1.13	13.9	S
(9,8)	1.15	28.1	S
(13,3)	1.15	10.2	S
(11,8)	1.29	24.8	M
(15,6)	1.47	16.1	M
(15,6)	1.47	16.1	M
(15,6)	1.47	16.1	M
(15,6)	1.47	16.1	M
(12,10)	1.49	27	S
(12,10)	1.49	27	S
(12,10)	1.5	27	S
(14,8)	1.51	21.1	M
(18,3)	1.54	7.6	M
(12,11)	1.56	28.6	S
(14,9)	1.57	22.8	S
(16,7)	1.6	17.2	M
(19,3)	1.61	7.2	S
(17,6)	1.61	14.6	S
(20,2)	1.65	4.7	M
(16,8)	1.66	19.1	S
(15,10)	1.71	23.4	S
(18,7)	1.75	15.7	S
(17,9)	1.79	19.9	S
(16,11)	1.84	23.9	S
(14,14)	1.9	30	M
(25,1)	2	1.95	M
(20,10)	2.07	19.1	S
(22,8)	2.11	14.9	S
(26,3)	2.16	5.4	S
(26,16)	2.22	22.2	S
(22,10)	2.22	17.8	M
(28,1)	2.23	1.7	M
(18,15)	2.24	27	M
(17,17)	2.3	30	M
(23,10)	2.3	17.2	S
(26,6)	2.31	10.2	S
(19,15)	2.31	26.1	S
(26,7)	2.36	11.6	S
(26,7)	2.36	11.6	S
(29,4)	2.37	6.4	S
(27,6)	2.39	9.83	M

(26,8)	2.41	13	M
(18,18)	2.44	30	M
(26,9)	2.47	14.3	S
(21,16)	2.52	25.5	S
(30,4)	2.52	6.2	S
(25,12)	2.56	18.5	S
(27,12)	2.71	17.5	M
(27,12)	2.71	17.5	M
(35,0)	2.74	0	S
(31,7)	2.75	10	M
(31,7)	2.75	10	M
(27,13)	2.76	18.6	S
(30,9)	2.77	12.7	M
(28,12)	2.79	17	S
(31,8)	2.79	11.2	S
(36,0)	2.82	0	M
(23,19)	2.85	26.9	S
(23,19)	2.85	26.9	S
(26,16)	2.88	22.2	S
(33,7)	2.9	9.4	S
(31,10)	2.9	13.5	M
(30,12)	2.94	16.1	M
(32,10)	2.98	13.1	S
(37,2)	2.98	2.6	S
(24,20)	2.99	27	S
(26,18)	3	24	S
(30,16)	3.12	20	S
(26,20)	3.13	25.7	M
(27,19)	3.14	24.3	S
(30,16)	3.17	20	S
(28,19)	3.21	23.7	M
(28,19)	3.21	23.7	M
(37,8)	3.25	9.6	S
(40,3)	3.26	3.6	S
(32,15)	3.26	18.2	S
(28,20)	3.27	24.5	S
(41,2)	3.29	2.4	M
(34,14)	3.35	16.4	S
(35,13)	3.36	15.2	S
(35,13)	3.37	15.2	S
(40,6)	3.39	6.9	S
(25,25)	3.39	30	M
(42,5)	3.5	5.6	S
(45,0)	3.52	0	M
(41,8)	3.57	8.8	M
(28,25)	3.6	28.1	M
(33,20)	3.63	21.9	S
(47,2)	3.76	2.1	M

(34,21)	3.77	22.2	S
(45,6)	3.78	6.2	M
(32,24)	3.81	25.3	S
(44,12)	4	11.7	S
(35,28)	4.28	26.3	S
(45,17)	4.35	15.4	S
(52,10)	4.51	8.6	M
(43,24)	4.61	20.7	S

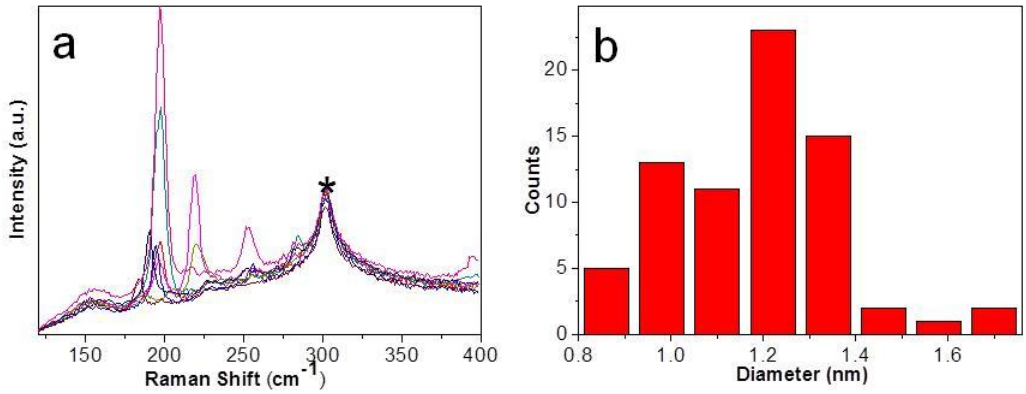

Figure S1. (a) Radial breathing modes (RBMs) in the Raman spectra of carbon nanotubes grown at 800 ^{o}C using CO as the carbon source ($\lambda_{excitation}$ = 633 nm), the marked peaks are originated from the substrate. (b) Diameter distribution of SWNTs deduced from the RBM frequencies (ω (cm^{-1}) = 248 cm^{-1}•nm/d (nm)), showing a mean diameter of 1.2 nm.

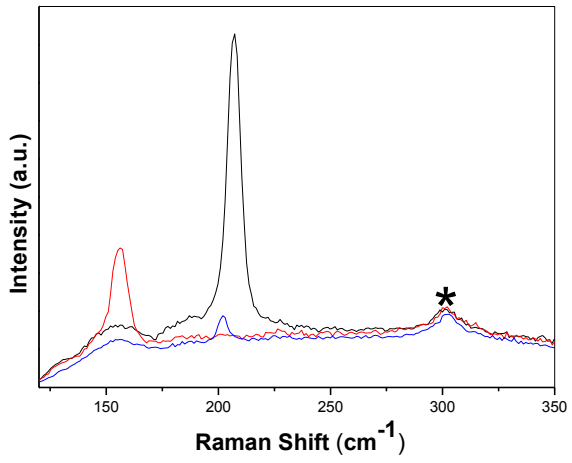

Figure S1. (a) RBMs in the Raman spectra of carbon nanotubes grown at 800 ^{o}C using CH_4 as the carbon source ($\lambda_{excitation}$ = 633 nm). The marked peaks are originated from the substrate.

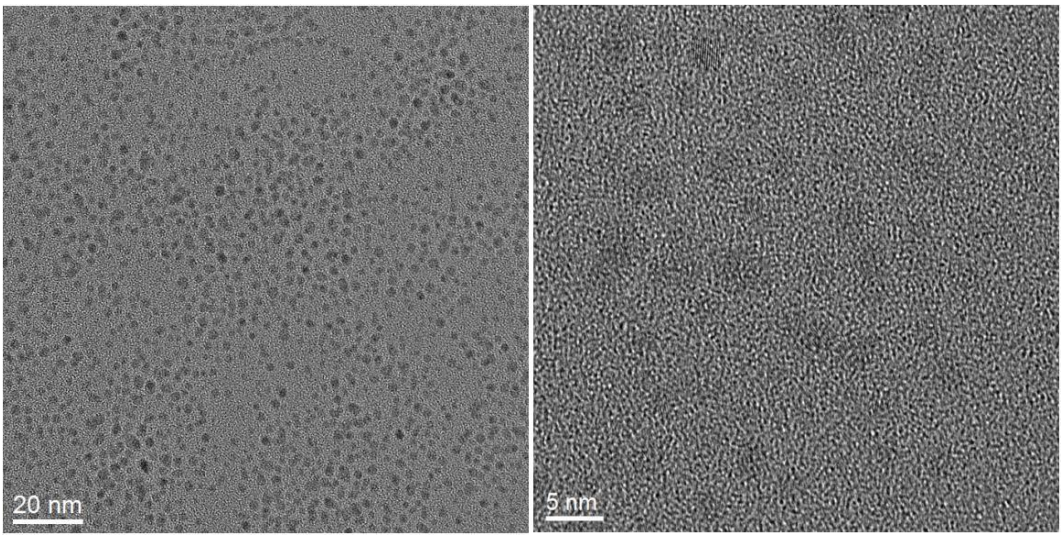

Figure S3. TEM images of synthesized Fe nanoparticles by microwave irradiation.

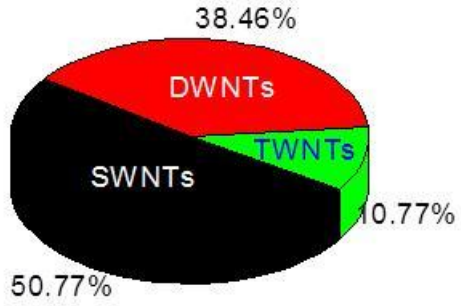

Figure S4. The wall number distribution of carbon nanotubes grown at 950 ^{o}C using CH_4 as the carbon source.

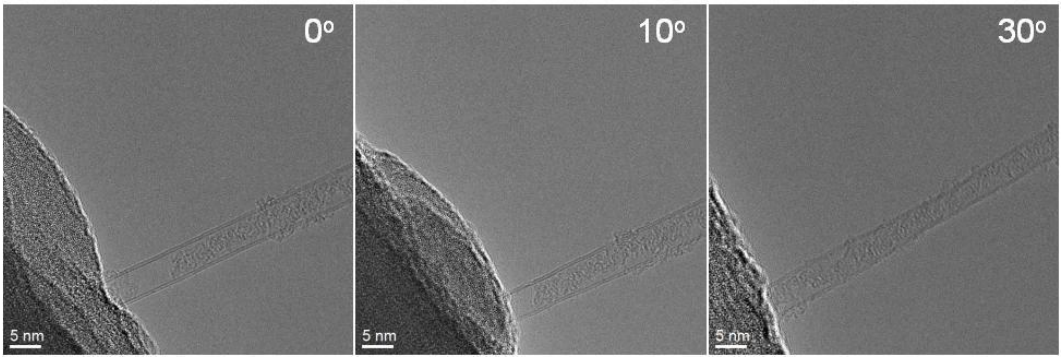

Figure S5. A series of TEM images of carbon nanostructures synthesized at 950 ^{o}C using CH_4 as carbon source obtained at different tilt angles.